

# We are IntechOpen, the world's leading publisher of Open Access books Built by scientists, for scientists

**4,800**

Open access books available

**122,000**

International authors and editors

**135M**

Downloads

Our authors are among the

**154**

Countries delivered to

**TOP 1%**

most cited scientists

**12.2%**

Contributors from top 500 universities



**WEB OF SCIENCE™**

Selection of our books indexed in the Book Citation Index  
in Web of Science™ Core Collection (BKCI)

Interested in publishing with us?  
Contact [book.department@intechopen.com](mailto:book.department@intechopen.com)

Numbers displayed above are based on latest data collected.

For more information visit [www.intechopen.com](http://www.intechopen.com)



---

# Surface Modification of CdSe and CdS Quantum Dots-Experimental and Density Function Theory Investigation

---

Liang-Yih Chen, Hung-Lung Chou, Ching-Hsiang Chen and Chia-Hung Tseng

Additional information is available at the end of the chapter

<http://dx.doi.org/10.5772/46516>

---

## 1. Introduction

Semiconductor nanocrystals (NCs), also referred to as semiconductor quantum dots (QDs), which are small compared to the bulk exciton radius have unique properties associated with the spatial confinement of the electronic excitations. These semiconductor QDs have discrete electronic states, in contrast to the bulk band structure, with an effective band gap blue shifted from that of the bulk. Due to their unique properties, QDs have been of great interest for fundamental research and industrial development in recent years [1-2]. The size-dependent optical properties of QDs have been actively studied during the pass decade. The synthesis and subsequent functionality of QDs for a variety of applications include photostable luminescent biological labels [3-8], light harvesters in photovoltaic devices [9-15] and as the emissive material in light-emitting devices (LEDs) [16-23]. They are also characterized by large surface to volume ratios. Unlike quantum wells and wires, experimental studies suggest that the surfaces of QDs may play a crucial role in their electronic and optical properties. However, these semiconductor QDs with large surface to volume ratios are metastable species in comparison to the corresponding bulk crystal and must be kinetically stabilized. The most common method to maintain their stability is by chemically attaching a monolayer of organic molecules to the atoms on the surfaces of QDs. These organic molecules are often called surfactants, capping groups, or ligands. In addition to the protection function, this monolayer of ligands on the surfaces of QDs provides the necessary chemical accessibility for the QDs by varying the terminal groups of the ligands pointing to the outside environment. For example, the QDs covered with hydrophobic ligands cannot be used directly in applications that require aqueous solubility or an effective charge transport property.

For both the protection and solubility function, the photoluminescence quantum yield (PL-QY) is another crucial factor for semiconductor QDs. The QDs have a large fraction of surface atoms because of their small volume; therefore, several inhomogeneous defect points occur on the large surface area. The processes that determine the luminescence QYs in semiconductor QDs have been investigated for several years. In this topic, the surface chemistry plays a crucial role in the manipulation of semiconductor QDs because it determines the dispersion interactions of the QDs in the medium, and high quantum yields and long term photostability can be achieved only through an improved understanding of surface recombination processes. Therefore, proper passivation of the surfaces of QDs is necessary to achieve a high PL-QY.

QDs of II-VI semiconductors have been extensively studied during the past two decades [24-30]. To date, the light-emitting core part of most QDs is cadmium selenide (CdSe), which can be prepared under mild conditions using well-known precursors. However, CdSe QDs have a spectral limitation at emission wavelengths shorter than 490 nm. To achieve high quantum efficiency in the blue region, cadmium sulfide (CdS) is a suitable candidate that can be prepared under mild conditions. Because the bulk CdS has an energy band gap of approximately 2.5 eV, it is easier to enable CdS QDs to emit blue light than the same sized CdSe. In connection with the improvement of the emission efficiency of CdSe and CdS QDs, several studies focused on the capping ligands introduced to the surfaces of CdS and CdSe QDs to study the variation of PL-QY [31-35]. In general, the usual method for surface modification of CdS QDs is to cap the synthesized CdS QDs with thiolate ligands during the growth period [36]. Uchihara et al. investigated the pH dependent photostability of thioglycerol-capped CdS (TG-CdS) and mercaptoacetate-capped CdS (MA-CdS) in colloidal solutions under stationary irradiation [37]. Because of the various charge properties of TG and MA, the carboxyl group of MA is neutralized by the addition of proton in the lower pH region, and the photostability decreases by lowering the pH of the solutions for MA-CdS; however, the photostability of TG-CdS are slightly influenced by the pH of the solution. Thangadurai et al. used 1,4-dithiothreitol (DTT), 2-mercaptoethanol (ME), cysteine (Cys), methionine (Meth), and glutathione (GSH) as ligands to cap the surfaces of CdS QDs to study the photo-initiated surface degradation [33]. It is noteworthy that the band edge emission of DTT capped CdS shifted to a higher energy, and this shift was in conformity with the lowest grain size. In addition, the intensity of the broadband related to the surface defect states of CdS QDs exhibited a reduced trend compared to the other samples. The surface coating with suitable thiol molecules can yield a lower grain size in the cubic phase and obtain excellent fluorescence properties with efficient quenching of the surface traps.

In contrast to the photochemical stability of thiol capped-CdS QDs, the photochemical instability of CdSe QDs capped with thiol molecules was reported by Peng et al. [34]. Based on their research, they proposed that the photochemical instability of CdSe QDs capped with thiol molecules included three distinguishable processes, as follows: (1) the photocatalytic oxidation of the thiol molecules on the surfaces of CdSe QDs; (2) the photooxidation of CdSe QDs; and (3) the precipitation of CdSe QDs. Thiols are the most widely used ligands for stabilizing semiconductors [38-39]. However, the stability of the

thiol-stabilized CdSe QDs is not satisfactory because of the photooxidation of the QDs-ligand complex using CdSe QDs as the photocatalysts. It is difficult to reproducibly apply chemical and biochemical procedures to these QDs because of their unstable nature. In addition to the use of thiol molecules to cap the surfaces of CdSe QDs, most researchers used various amines as ligands to modify the optical properties of CdSe QDs [40-44]. Talapin et al. synthesized CdSe QDs in a three-component hexadecylamine (HDA)-trioctylphosphine oxide (TOPO)-trioctylphosphine (TOP) mixture [35]. The room temperature PL-QY of as-synthesized CdSe QDs without adding HDA was in the range of 10-25%. However, the PL-QY of CdSe QDs can be improved substantially by surface passivation with HDA molecules. This indicates that PL efficiency losses are caused by insufficient passivation of the surface traps. Murray et al. examined the effect of the surface modification of CdSe QDs on the optical properties [45]. They interpreted the substantial increase in PL intensity following the addition of HDA molecules as the elimination of nonradiative decay pathways. Similar results were reported by Bullen and Mulvaney with primary, secondary, and tertiary amine [41].

Two types of alkylamine (*n*-butylamine (*n*-BA) and *n*-hexylamine (*n*-HA)) and oleic acid (OA) were used to modify the surfaces of the CdS and CdSe nanocrystals. To understand the changes of optical properties of un-modified QDs and surface modified QDs, PL spectra and PL-QY were used to characterize the emission peak position and emission efficiency after surface modification of these ligands for CdSe and CdS QDs. The PL decay kinetics for these ligand capped-QDs systems were followed by time-resolved photoluminescence (TRPL), and the spectra were analyzed in regard to a biexponential model to identify two lifetime values, that is, shorter-lifetime ( $\tau_s$ ) and longer-lifetime ( $\tau_L$ ). The detailed mechanism was studied by density function theory (DFT) simulation to demonstrate the binding energy and charge analyses of CdS or CdSe QDs with *n*-BA, *n*-HA, and OA.

## 2. The surface modification of CdS and CdSe QDs via organic ligands

The capping of CdS and CdSe QDs consisting of semiconductor cores surrounded by organic ligands has attracted considerable interest for applications in materials science and nanotechnology [46-48]. Although these studies enabled syntheses of stable capping semiconductor QDs with various sizes, shapes, and compositions, few studies have been conducted on the surface structures and properties of capping ligands. Information regarding the nature and chemical properties of the binding between QDs and their ligands is limited. However, compared to atoms on the flat surface of bulk substrates, the binding abilities of atoms on curved surfaces may be affected by their diverse structural environments and size-dependent electron configuration. In this study, the synthesis of CdS and CdSe QDs was conducted in a noncoordinating solvent using 1-ODE. The CdO (0.16 mmol) was mixed with 0.7 mmol OA and 4.8 g of 1-ODE in a 25 mL three-neck flask. The mixture was heated to 300 °C under Ar flow for 30 min, and subsequently injected with Se stock solution (0.1 mmol of S or Se powder dissolved in 0.62 mmol of TBP and 1 g of ODE). The solution mixture was cooled, and the nanocrystals were allowed to grow at 260 °C to

reach the desired size, as determined by UV-visible absorption. To monitor the growth of QDs, a small amount of the sample (approximately 0.2 mL) was obtained through a syringe and diluted to exhibit an optical density between 0.1 and 0.2 by the addition of anhydrous toluene. The resulting CdS and CdSe QDs were suspended in toluene, and the unreacted starting materials and side products were removed by extraction and precipitation procedures. Size sorting was not performed in any of the samples. An aliquot of CdS or CdSe QDs solution was diluted with toluene to yield an optical density of approximately 0.1 at a wavelength of 350 nm (the excitation wavelength of PL). A 3 mL portion of the nanocrystals solution was mixed with various capping molecules at a fixed concentration of 5 mM for surface modification. The solution mixture was stirred in the dark at room temperature for 1 h. The CdS and CdSe QDs were subsequently precipitated with methanol and re-dispersed in toluene for characterization of the change of PL quantum yield by UV/vis absorption and photoluminescence spectroscopy.

Figure 1 shows the transmission electron microscopic (TEM) images of the as-grown CdSe and CdS QDs synthesized by the non-coordinate method. It shows that the material has a uniform size distribution and regular shape with 5 nm and formed close-packed arrays.

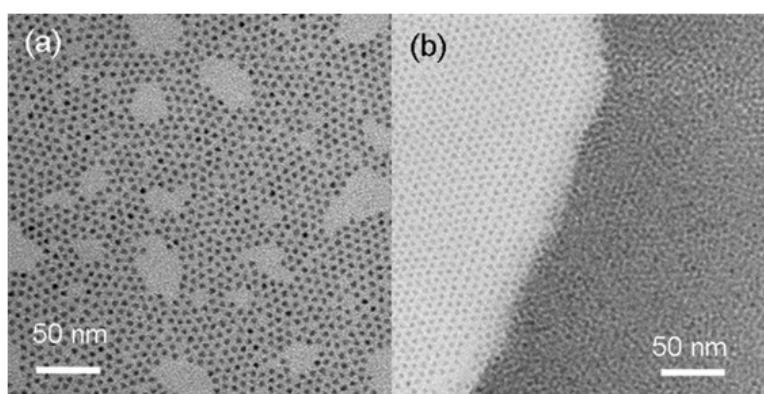


**Figure 1.** Transmission electron microscopic images of samples of (a) CdSe QDs; (b) CdS QDs.

The absorption and PL spectra of the CdSe QDs varying with growth time are shown in Figure 2. The luminescence spectra from these CdSe QDs are symmetric and narrow. However, the PL quantum yields decreased in conjunction with the growth time to 5%, as shown in Figure 2(c). The absorption and PL spectra of CdS QDs recorded for samples grown at various times are shown in Figure 3. The PL-QY increased rapidly in conjunction with the growth time initially and reached a steady value of approximately 60% after 200 s. The increasing PL-QY with crystal growth for CdS QDs exhibited contrasting behavior to several other QDs, such as CdSe, which exhibited a decreasing PL QY with crystal growth time [49]. A characteristic peak for CdS QDs was not observed in the UV and PL spectra in the initial 60 s after S precursor injection to the Cd<sup>2+</sup> solution. The UV absorption spectrum and the narrow emission peak with full-width at half maximum (approximately 21 nm) were observed after 60 s reaction. This behavior can be attributed to the slow growth of CdS QDs in the initial period, and their size was too small in this time domain for identification by the spectroscopy of UV-visible absorption and PL emission. Therefore, because of the

slow growth process in the formation of CdS QDs, high quality QDs with large quantities of radiative surface-states with low nonradiative surface quenching defects can be obtained with the increase in PL-QY in conjunction with the growth time.

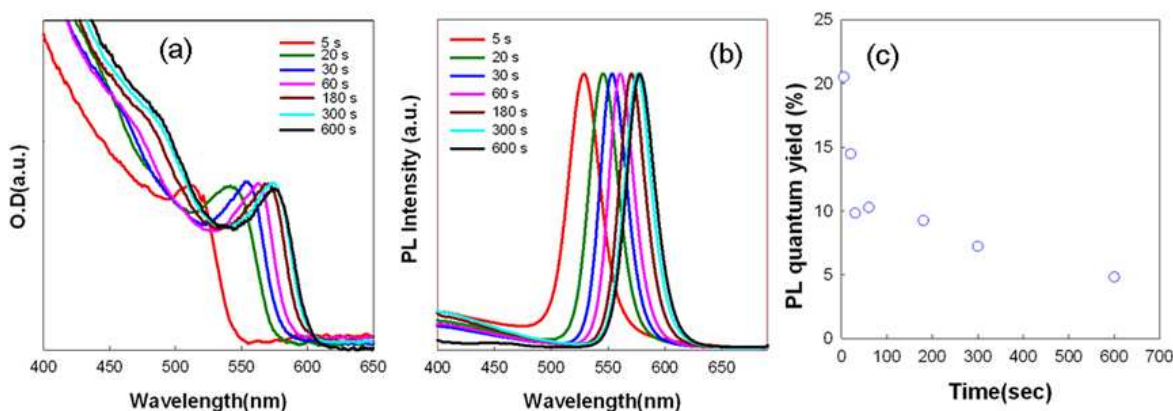


**Figure 2.** Temporal evolution of (a) UV-vis; (b) PL spectra and (c) PL quantum yield of a growth reaction of CdSe QDs.

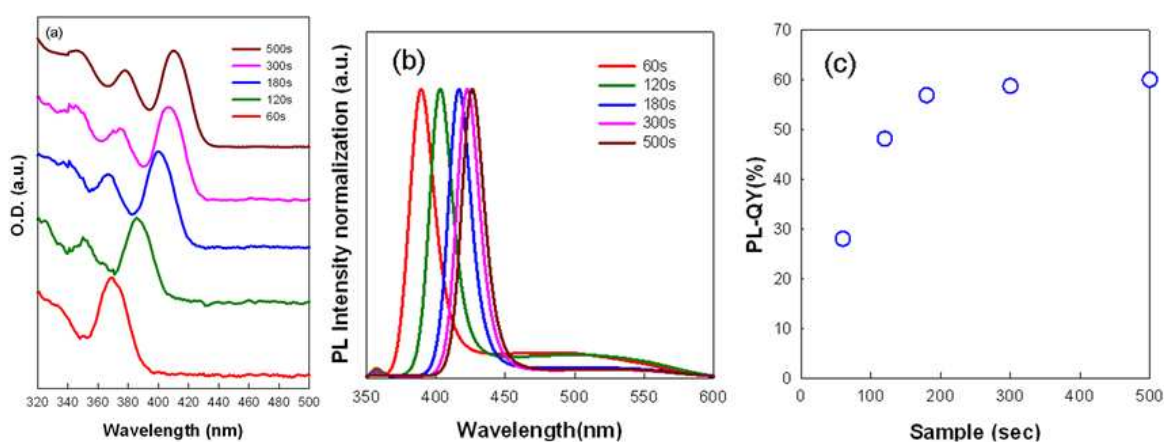


**Figure 3.** Temporal evolution of (a) UV-visible spectra; (b) PL spectra and (c) PL quantum yield of a growth reaction of CdS QDs.

Based on these observations, the control of the surface, probably a reconstructed surface of QDs, may be crucial for controlling and improving their PL properties. To understand the changes in the optical properties of the CdSe and CdS QDs upon modification by the capping ligands, *n*-BA, *n*-HA, and OA were added to a solution of as-grown CdSe and CdS QDs solution, and the PL and the UV/vis spectra were recorded before and after the addition. The PL spectra and the quantum yields of the CdSe QDs modified by *n*-BA, *n*-HA, and OA are shown in Figure 4. As shown in Fig. 4, the positions of the luminescence emission peaks of the ligand-modified CdSe QDs shifted to lower wavelengths for the three capping molecules compared to the as-grown CdSe QDs. Moreover, Figure 4(b) shows that the PL quantum yield increased to 45% and 61% for the amines *n*-BA and *n*-HA capping CdSe QDs, respectively, whereas OA capping of CdSe QDs exhibited a decrease to 5%. For

ligand capping of CdS QDs, the PL spectra and the QYs of the CdS QDs modified by *n*-BA, *n*-HA, and OA are shown in Figure 5. As shown in Figure 5(a), the PL intensity was decreased substantially by the additives in the entire wavelength region, whereas the PL spectral maximum occurred at the same wavelength for all systems. Figure 5(b) shows that the PL QY of CdS QDs decreased from 60% to 6% and 3% for *n*-BA and *n*-HA, respectively, whereas OA exhibited a decrease to 2%. Compared to the case of CdSe QDs, the three organic additives in this study exhibited contrasting behavior for the CdS QDs system.

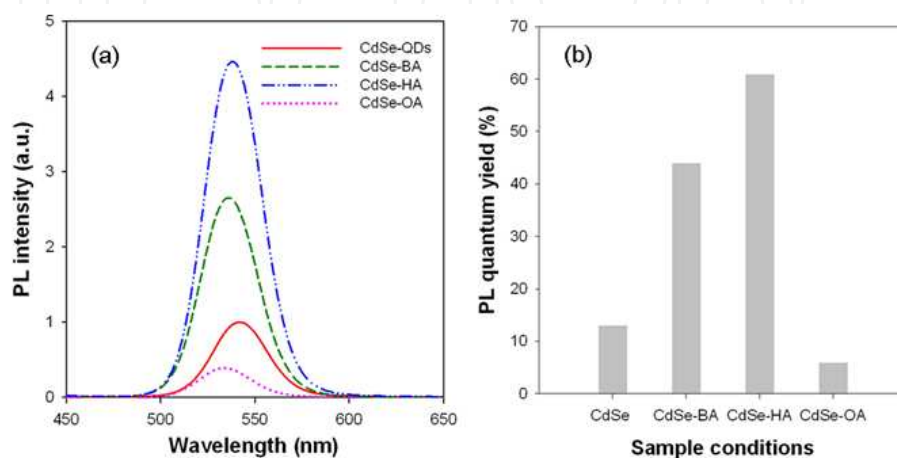


**Figure 4.** (a) Room temperature PL spectra of as-grown, *n*-BA, *n*-HA and OA modified CdSe QDs; (b) The corresponding PL quantum yield variety of CdSe QDs after capping ligand modification.

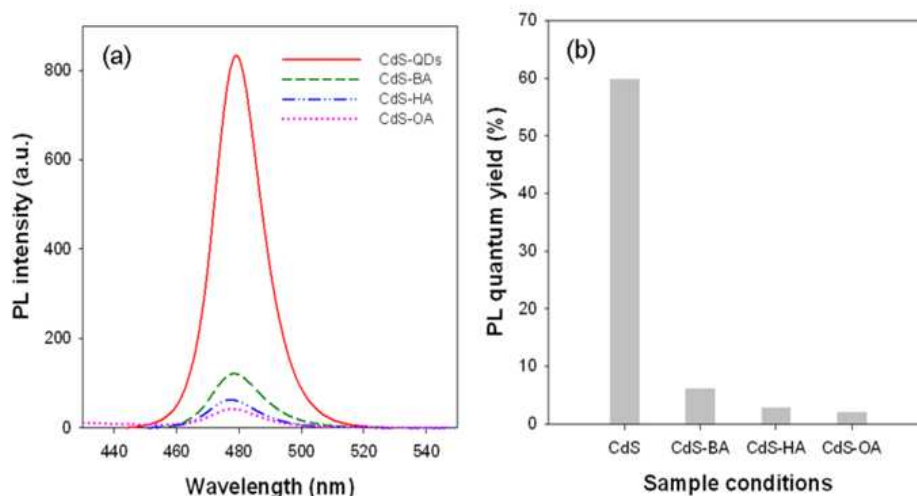


**Figure 5.** (a) Room temperature PL spectra of as-grown, *n*-BA, *n*-HA and OA capping molecule modified CdS QDs; (b) PL quantum yield of CdS QDs versus capping ligands.

Generally, it is believed that the capping ligands effectively passivate the surface states and suppress the non-radiative recombination at surface vacancies, leading to enhanced PL quantum yield. However, among the three capping agents in the case of CdSe QDs, the OA ligand exhibited contrasting behavior. In addition, the three ligands were used to quench the emission properties of CdS QDs. Generally, the relaxation process of QDs is radiative

recombination. Otherwise, competing radiation-less relaxation processes are used, including carrier trapping at QD defects, charge transfer between QDs and ligand-based orbitals, and inter-QDs energy transfer. The observations in this study clearly indicate that the passivation effect of the capping ligands for CdSe and CdS QDs are more complex, indicating the requirement for a careful examination of the photo-induced charge transfer between CdSe QDs and the capping ligands.

To resolve the various behaviors of CdS QDs, time-resolved photoluminescence (TRPL) was used to probe the decay kinetics of the exciton emission of bare QDs and ligand capping QDs by *n*-BA, *n*-HA, and OA molecules. Because of the high sensitivity of TRPL for ensemble and single particle PL analysis, it is often used to determine the transient population of one or more radiative excited states [50].

### 3. The study of time resolved photoluminescence technique on surface modification of CdS and CdSe QDs.

For TRPL analysis, this study used a system with a single picosecond diode laser driver with a 375nm laser head (integrated collimator and TE cooler for temperature stabilization was integrated by Protrustech Co., Ltd). An Andor iDus CCD with 1024 × 128 pixels was used to obtain the PL signal and the Pico Quant PMT Detector head with 200–820 nm and <250 ps IRF was integrated to obtain the TRPL signal. A theoretical model with multi-exponential analysis is often used to determine the lifetime of QDs by PL decay data. Typically, the feature of the decay of the PL intensity for QDs is a universal occurrence of a biexponential time distribution in the radiative lifetime, as shown in the following equation,

$$I(t) = A_S e^{-t/\tau_S} + A_L e^{-t/\tau_L} \quad (1)$$

where  $\tau_S$  and  $\tau_L$  represent the shorter lifetime and longer lifetime, respectively, and  $A_i$  ( $i = S, L$ ) is the amplitude of the components at  $t = 0$ . The shorter lifetime is on a time scale of several nanoseconds, and the longer lifetime is on a time scale of tens of nanoseconds. The shorter lifetime is generally attributed to the intrinsic recombination of initially populated internal core states; however, the possible origin of the longer lifetime remains relatively uncertain [51-53]. Recently, Xiao et al. reported that the longer lifetime component in the PL decay is caused by the radiative recombination of electrons and holes on the surface involving surface-localized states [53]. For QDs with high PL-QY, the amplitude  $A_L$  with longer lifetime dominates the total PL. In other words, electrons and holes have an increased probability to be presented on the surfaces of QDs with high QY to contribute to this surface-related emission with a longer lifetime.

The representative PL decay curves recorded for the bare CdSe and CdS QDs and their surfaces treated by *n*-HA, *n*-BA, and OA molecules are shown in Figure 6. All of the decay curves were fitted to the biexponential equation (1). The resulting decay time constants ( $\tau_i$ ), their fraction contribution ( $Y_i$ ), average decay lifetimes ( $\langle \tau \rangle$ , calculated from (2)), the values of the goodness-of-fit parameter ( $\chi^2$ ), and the quantum yield ( $\Phi$ ) are listed in Table 1 for each system. The criteria for an acceptable fit have been justified in the previous article [54].



$$\langle \tau \rangle = \frac{\sum_i A_i \tau_i^2}{\sum_i A_i \tau_i} \quad (2)$$

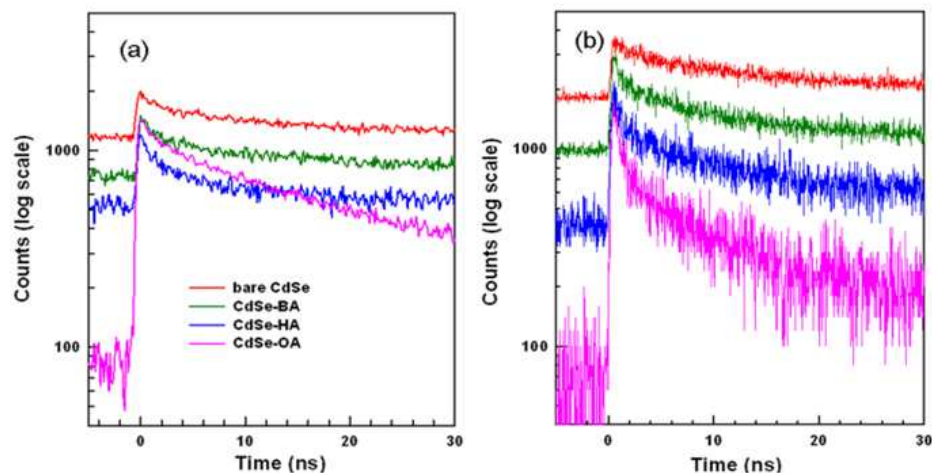


**Figure 6.** PL decay spectra for (a) bare CdSe QDs and surface modified by *n*-BA, *n*-HA and OA; (b) bare CdS QDs and surface modified by *n*-BA, *n*-HA and OA.

Sample ID	YS (%)	$\tau_S$ (ns)	YL (%)	$\tau_L$ (ns)	$\langle \tau \rangle$ (ns)	$\chi^2$	QY (%)
CdSe	62	2.93	38	16.99	13.90	0.968	13
CdSe-BA	44	2.69	56	22.87	21.16	0.931	44
CdSe-HA	36	2.50	64	28.52	27.30	1.021	61
CdSe-OA	89	0.64	11	10.76	7.47	0.926	6
CdS	43	2.27	57	22.60	21.18	0.988	60
CdS-BA	63	0.90	37	16.61	15.30	0.977	6.2
CdS-HA	75	0.88	25	18.78	16.61	0.961	3.2
CdS-OA	93	0.07	7	12.46	11.60	1.035	2.2

<sup>a</sup>PL decay was analyzed using biexponential model described by  $I(t) = A_S e^{-t/\tau_S} + A_L e^{-t/\tau_L}$  and the fraction

contribution was calculated by  $Y_i = \frac{A_i}{\sum_i A_i} \times 100\%$ .

**Table 1.** Fitted PL decay lifetime components.<sup>a</sup>

As shown in Table 1, for bare CdSe and CdS QDs,  $\tau_S$  equals to 2.93 ns and 2.27 ns, and  $\tau_L$  equals to 16.99 ns and 22.60 ns. The value of  $\tau_S$  for the short lifetime constant is consistent with the theoretical value of approximately 3 ns, which was calculated by considering the screening of the radiating field inside the QD [55]. Moreover, for the bare CdS QD samples with 60% QY, the amplitude of  $A_L$  with a longer lifetime accounts for nearly 57% of the total PL. Similar results were observed in the capping ligands for modified CdSe QDs. This larger share of the longer lifetime component is a clear indication of major surface-related emission

caused by the radiative recombination of charge carriers involving surface states. Although it is difficult to identify the real origin for such radiative recombination through surface state centers in this stage, it may result from the net residual charges on atoms of CdSe and CdS QDs caused by the bonding of Cd-Se and Cd-S and the nearest neighboring atoms in the crystal lattice.

#### 4. The investigation of density function theory (DFT) on capping CdS and CdSe QDs.

Here, we proposed to use the density function theory (DFT) calculations result to provide atomistic information on the adsorption energy and charge transfer of small QDs capped by different types of ligands. Theoretical modeling could provide valuable insight in atomic scale. Unfortunately, efforts in this field have been rather limited due to the high computational cost and uncertainty related to the chemical composition and morphology of the nanocrystals. Early theoretical studies of QDs simulated the surface by assuming an infinite potential barrier around the QDs. [56]. More sophisticated models of capping QDs have represented the QD core through the bulk atoms using semiempirical tight-binding [57] and pseudopotential [58] approaches, while the passivating molecules have been modeled through either single oxygen atoms or simplified model potentials [59]. Any realistic model, however, has to explicitly describe bonding between the QD and the ligands, which is lacking from the approaches mentioned above. First-principle quantum-chemical methods, such as density functional theory (DFT), are able to provide this information with a reasonable level of accuracy. Unfortunately, DFT is numerically expensive. Therefore, most DFT calculations simulate the core atoms of QDs on the basis of bulk structures, while dangling bonds on the surface are artificially terminated with covalently bonded hydrogen atoms [60-61]. Only a few reports have focused the specifics of the adsorption energies and charge transfer of small cluster of QD interacting with ligand molecule. [46, 62]

The experimentally studied QDs retained the original crystal structure in the core. Figure 7 shows the construction of CdSe from a zinc blended lattice with bulk Cd-Se bond lengths. The analogous construction of CdSe clusters from the bulk semiconductor has been used in theoretical studies. [46, 63-65]. In addition to the uncapped ("bare") CdSe and CdS, we simulated clusters with ligands attached to the surface of the QDs. The selected capping groups, that is, *n*-butylamine (*n*-BA), *n*-hexylamine (*n*-HA), and oleic acid (OA) were used as ligands for the QDs. Thus, our simulations allowed us to study the interaction between ligand binding to Cd atoms, and the effects of these differences on the adsorption energy and optical response of the ligand capping of CdSe and CdS QDs.

In the previous studies have shown computationally that the dominant binding interaction occur between N atoms of the ligand and Cd atoms on the QD surface. We start our modeling with constructing three systems, Cd<sub>4</sub>Se<sub>4</sub>, Cd<sub>4</sub>Se<sub>4</sub>HA, Cd<sub>4</sub>Se<sub>4</sub>BA, Cd<sub>4</sub>Se<sub>4</sub>OA, Cd<sub>3</sub>S<sub>5</sub>, Cd<sub>3</sub>S<sub>5</sub>HA, Cd<sub>3</sub>S<sub>5</sub>BA, Cd<sub>3</sub>S<sub>5</sub>OA, and CdSe(111) slab (see Figure 8 (b) and (c)). The ligands were attached to the most chemically active surface atoms (all 2-coordinated Cd atoms on the

cluster surface) as described the previous studies [49, 66]. Recent experiments have shown that such small “magic”-size QDs with diameter than  $\sim 2\text{nm}$  demonstrate great stability, the controllable size and shape, and reproducible optical properties, including an efficient blue-light emission [64]. The  $\text{Cd}_{33}\text{Se}_{33}$  “magic” structure with diameter of 1.3 nm has been experimentally shown to be very stable [64], while it is the smallest cluster that supports a crystalline-like core-shell.

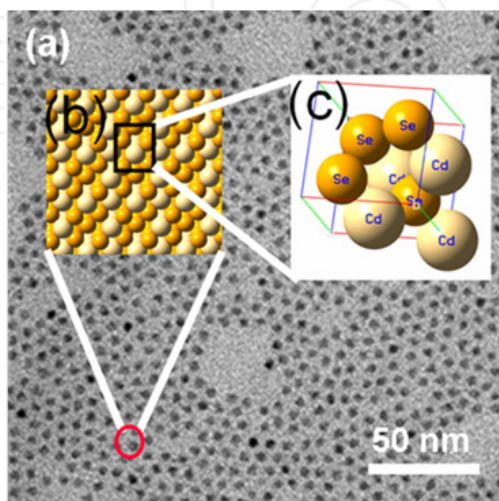


**Figure 7.** The (a) TEM image of a sample of CdSe QDs; (b) Snapshot of CdSe  $5 \times 5$  supercell; (c) unit cell of CdSe lattice.

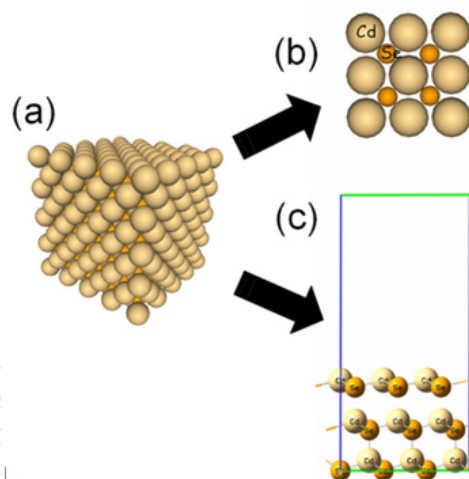


**Figure 8.** (a) The supercell of QD. (b) A finite cluster is used to model the surface (in the cluster approach) (c) A well-defined, finite vacuum space is used to model the surface (in the slab approach).

Two systems were applied in this work. To save computation resources, the  $\text{Cd}_4\text{M}_4$  ( $\text{M} = \text{Se}$  and  $\text{S}$ ) cluster is a reliable model for quantum-chemical studies of physical chemistry properties of CdSe and CdS QDs. The system requires reasonable computational efforts for atomistic modeling based on DFT, even when it is passivated with multiple ligands. A cluster model was used to simulate the interaction between the ligand and QD. This cluster was cut from the CdSe supercell optimized by DFT. Figure 9 shows the cluster model, in which the formula of the cluster is  $\text{Cd}_4\text{Se}_4$  and the nitrogen atoms are bonded on the Cd atoms.

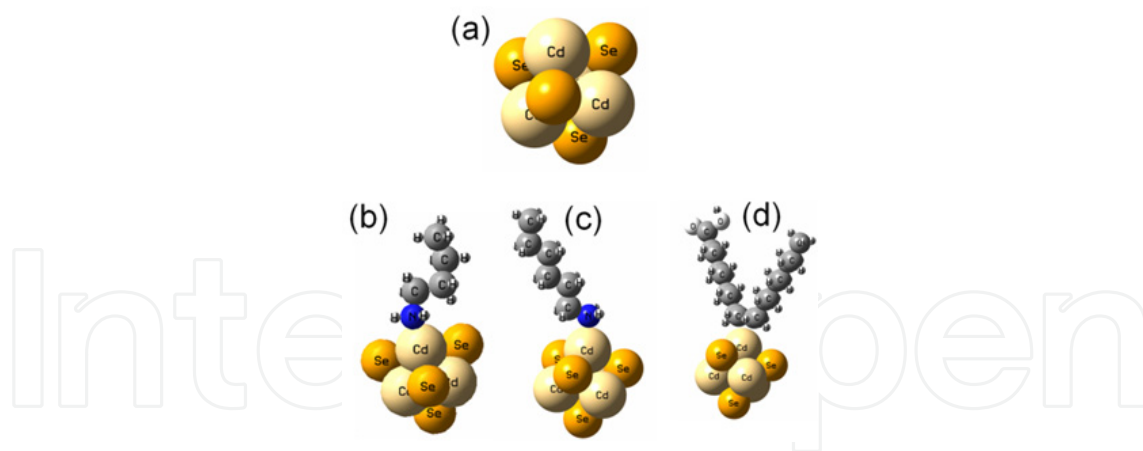


**Figure 9.** The optimized geometry of (a) CdSe cluster, (b) CdSe with *n*-BA, (c) CdSe with *n*-HA, and (d) CdSe with OA ligand.

#### 4.1. CdSe

As the CdSe nanostructures were modified by the capping ligands, the capping effect of *n*-HA, *n*-BA, and OA was derived in regard to the binding energy ( $E_b$ ) of capping molecules on a CdSe cluster and the residual surface charge on the capping molecules and the CdSe with the help of ab initio simulations. In the DFT calculation, amine and carboxylic acid were considered the main functional groups in obtaining the  $E_b$  on CdSe. To simplify the simulations, we used a Cd<sub>4</sub>Se<sub>4</sub> cluster to model the functional groups (Figure 9). During the simulations, the capping molecules were assumed to adsorb and attach on the CdSe cluster, and the binding energies of *n*-BA, *n*-HA, and OA ligands were computed using DFT simulations of an isolated cluster with a single ligand molecule. Representative snapshots for each of the capping ligands adsorbed on an isolated CdSe cluster are shown in Figure 9(b)-(d). The binding energy,  $E_b$ , was defined as the sum of interactions between the capping molecule and cluster atoms, and was derived as  $E_b = E_{total} - E_{CdSe} - E_{capp}$ , where  $E_{total}$ ,  $E_{CdSe}$  and  $E_{capp}$  are the total energy of the system, cluster energy, and capping molecule energy, respectively. The negative sign of  $E_b$  corresponds to the energy gain of the system because of ligand adsorption.

Table 2 lists the  $E_b$  values calculated for the three capping ligands. We verified that the main contribution to the  $E_b$  resulted from the interactions of the CdSe with the capping ligands through the charges on the CdSe and the ligand functional groups. The negatively charged atoms of amines adsorbed on the CdSe cluster without changing the surface structure substantially. The *n*-BA and *n*-HA adsorbed exclusively through its nitrogen atom with  $E_b$  values of  $-0.99$  and  $-0.93$  eV for CdSe-BA and CdSe-HA, respectively. Conversely, OA yielded an  $E_b$  of  $-0.21$  eV for a CdSe cluster-OA combined with the conjugated bond (C=C) of the alkyl chain adsorbed on CdSe. Our attempts for a CdSe cluster-OA combined with carboxyl function group adsorbed on CdSe resulted in high energy and an unstable configuration with continuously varying distance between the reactive centers. This occurred because, according to the well-known hard and soft acids and bases theory [67], the Cd<sup>2+</sup> and Se<sup>2-</sup> soft ions cannot interact with hard -COOH of OA, as suggested by Chen et

al. [68]. The charge analysis showed that the charge transfer between OA and CdSe was small.

CdSe		CdS	
ligand	$E_b$ (eV)	ligand	$E_b$ (eV)
( <i>n</i> -BA) $C_4NH_2$	-0.93	( <i>n</i> -BA) $C_4NH_2$	-0.71
( <i>n</i> -HA) $C_6NH_2$	-0.99	( <i>n</i> -HA) $C_6NH_2$	-0.84
OA	-0.21	OA	-0.13

**Table 2.** Binding Energies ( $E_b$ ) of different ligands on CdSe and CdS QD

Puzder et al. obtained ca. 0.91 eV from DFT calculations for trimethylamine on a (CdSe)<sub>15</sub> NC [46]. Similar values (0.89-1.02 eV) have been reported in the DFT study of amines at a CdSe surface [69]. Our results for organic amines are in good agreement with these values. It must be noted that the more negative the  $E_b$  value the stronger is the adsorption. Indeed, in the simulation work, the more negative  $E_b$  value was used as optimum to represent the adsorption strength of the functional group on a given cluster, when several other possible configurations for the adsorption on the CdSe cluster existed. Now, concerning the three capping ligands, the higher negative  $E_b$  values for the amine derivatives clearly indicate a stronger adsorption of these compounds on CdSe than the OA acid ligand with a lesser negative  $E_b$ .

The Bader charge analyses were carried out for CdSe, *n*-BA, *n*-HA, OA, CdSe-BA, CdSe-HA and CdSe-OA to examine the variations in  $E_b$  in terms of charge transfer between CdSe and capping molecules, and the charge results are listed in Table 3. In CdSe-BA and CdSe-HA systems, the charge of selenium was increased from 6.614 e (for the bare CdSe) to 6.696e and 6.700e, respectively. This is quite reasonable since the donation of charge of nitrogen atom of capping molecules to Se would easily occur. On the other hand, in CdSe-OA system, the charge of selenium atom was increased to 6.637 e lesser than that of selenium atom in CdSe-BA and CdSe-HA systems.

The charges for Cd in CdSe-BA, CdSe-HA, and CdSe-OA exhibited a decrease from 11.404e for a bare CdSe, indicating a net electron transfer from Cd atom to Se for the three capping molecules. Cd has lower electronegativity (1.7) than that of nitrogen (3.0); therefore, greater electron donation occurs to Se from the N atom of the capping molecules than that from Cd. Although the amine molecules adsorb strongly with a facile electron donation from their “-NH<sub>2</sub>” functional group to Se of CdSe nanocrystals (with higher  $E_b$  values), the conjugated bond (C=C) of OA forms weak bonding with CdSe and lowers the capping effect of the molecule (with lower  $E_b$  values). In addition, the OA molecule with linear carbon-carbon structure can easily form a dense and stable cover layer on the surface of CdSe, thereby preventing other molecules from approaching the CdSe QDs [68]. Moreover, the structure of an OA molecule has large stereo-hindrance. All of these factors reduce the effective bonding between the OA molecule and CdSe considerably. Therefore, this study demonstrated that the improved charge transfer of amine-capped CdSe is mainly caused by the higher value of

the Bader charge, implying a larger charge donation than OA, and the modification of CdSe QD by molecular capping plays a vital role in improving the CdSe charge donation.

System	Charge(e)	Charge difference(e)	System	Charge(e)	Charge difference(e)
CdSe	Se:6.614 Cd: 11.404		CdS	S:6.723 Cd: 11.227	
BA	N: 7.787		BA	N: 7.787	
HA	N: 7.801		HA	N: 7.801	
OA	O: 7.921		OA	O: 7.921	
CdSe-BA	Se: 6.696	Se: 6.614-6.696 = -0.082	CdS-BA	S: 6.763	S: 6.723-6.763 = -0.040
	Cd: 11.388	Cd: 11.404-11.388 = + 0.016		Cd: 11.194	Cd: 11.227-11.194 = + 0.033
	N: 7.561	N: 7.787-7.561 = +0.226		N: 7.764	N: 7.787-7.764 = +0.023
CdSe-HA	Se: 6.700	Se: 6.614-6.700 = -0.086	CdS-HA	S: 6.775	Se: 6.723-6.775 = -0.052
	Cd: 11.375	Cd: 11.404-11.375 = +0.029		Cd: 11.207	Cd: 11.227-11.207 = +0.020
	N: 7.561	N: 7.801-7.561 = +0.24		N: 7.791	N: 7.801-7.791 = +0.010
CdSe-OA	Se: 6.637	Se:6.614- 6.637 = -0.023	CdS-OA	S: 6.727	S: 6.723- 6.727 = -0.004
	Cd: 11.267	Cd: 11.404- 11.267 = +0.137		Cd: 11.184	Cd: 11.227- 11.184 = +0.043
	O: 7.906	O: 7.921-7.906 = +0.015		O: 7.900	O: 7.921-7.900 = +0.021

**Table 3.** Charge transfer between CdSe and CdS and ligands

## 4.2. CdS

Surface modification of CdS nanostructures by the organics was treated in regard to the adsorption of *n*-HA, *n*-BA, and OA, and the corresponding binding energy ( $E_b$ ) of organic molecules and the residual surface charge on the organic molecules and the CdS were calculated with the help of ab initio simulations. Amine and carboxylic acid were considered the main functional groups for adsorption. A sulfur-rich structure on the surface (Cd : S=1 : 1.3) was identified through XPS analyses of the CdS QDs. To simplify the simulations, we used a Cd<sub>3</sub>S<sub>5</sub> cluster to model its interaction with the functional groups (Figure 10(a)). During simulations, the organic molecules were assumed to adsorb and attach on the CdS cluster, and the binding energies of *n*-BA, *n*-HA, and OA ligands were computed using DFT simulations of an isolated cluster adjoined with a single ligand molecule. Representative snapshots for each of the adsorbed molecules on an isolated CdS cluster are shown in Figure 10(b)-(d). The binding energy,  $E_b$ , was defined as the sum of interactions between the organic molecule and cluster atoms, and was derived as  $E_b = E_{total} - E_{CdS} - E_{capp}$ , where  $E_{total}$ ,  $E_{CdS}$  and  $E_{capp}$  are the total energy of the system, cluster energy, and organic molecule energy, respectively. The negative sign of  $E_b$  corresponds to the energy gain of the system caused by ligand adsorption.

The  $E_b$  values calculated for the three organic ligands are listed in Table 3. The main contribution to  $E_b$  resulted from the interactions of the CdS with the organic molecules

through the charges on the CdS and the ligand functional groups. Negatively charged atoms of amines adsorbed on the CdS cluster without changing the surface structure substantially. The *n*-BA and *n*-HA adsorbed exclusively through its nitrogen atom. The adsorbed amines on the CdS clusters produced binding energies of  $-0.71$  and  $-0.84$  eV for CdS–BA and CdS–HA, respectively. Conversely, the  $E_b$  of  $-0.13$  eV was small for the CdS–OA system with the conjugated bond (C=C) of the alkyl chain of OA adsorbed on CdS. Our attempts for a CdS cluster–OA with carboxyl function group adsorbed on CdS resulted in a high energy and unstable configuration with continuously varying distance between the reactive centers. This occurred because, according to the well-known hard and soft acids and bases theory, [67], the  $\text{Cd}^{2+}$  and  $\text{S}^{2-}$  soft ions cannot interact with hard  $-\text{COOH}$  of OA, as suggested by Chen et al. [68]. The more negative the  $E_b$  value, the stronger the adsorption. In the simulation, the final adsorption configuration with a more negative  $E_b$  value was selected as the optimal configuration, and its  $E_b$  value represented the adsorption strength of the functional group on a specified cluster when several other possible configurations for the adsorption on the CdS cluster were available. Strongly adsorbed organic additives generally exhibit higher binding energies of approximately  $-1.0$  eV. Therefore, the binding energy values obtained for the organics in this study indicate that the amines *n*-BA ( $-0.71$  eV) and *n*-HA ( $-0.84$  eV) adsorbed moderately, whereas the carboxylic acid OA ( $-0.13$  eV) adsorbed weakly on CdS QDs. Weak adsorption of OA can also be expected, because the OA molecule with a linear carbon-carbon structure can easily form a dense and stable cover layer on the surface of CdS, as reported for CdSe[68], thereby preventing other molecules from approaching the CdS QDs. Moreover, the structure of an OA molecule has a large stereo-hindrance. These factors reduce the effective bonding between the OA molecule and CdS considerably.

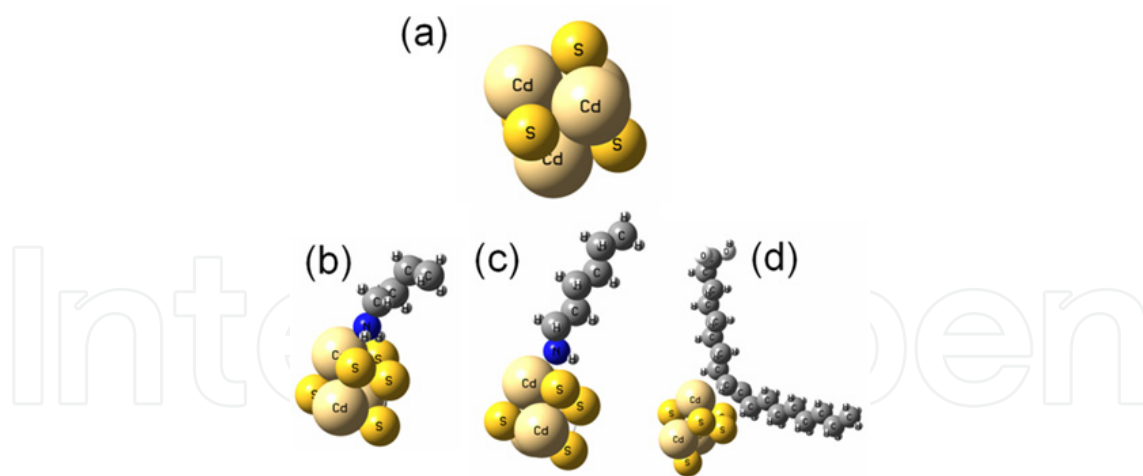


**Figure 10.** The optimized geometry of (a) CdS cluster; (b) CdS with *n*-BA; (c) CdS with *n*-HA, and (d) CdS with OA ligand.

Bader charge analyses were performed for CdS, *n*-BA, *n*-HA, OA, CdS-BA, CdS-HA, and CdS-OA to examine the variations in  $E_b$  in regard to charge transfer between CdS and organic molecules; the charge results are listed in Table 2. For example, in the typical CdS-BA system, the negative charge on S increased from  $-6.723e$  (for the bare CdS) to  $-6.763e$  (net negative charge gain  $-0.040e$ ) upon BA adsorption, which was caused by the donation

of electrons from the N atom of the amine to S, with a loss of negative charge on N from  $-7.787e$  (for BA molecule) to  $-7.764e$  (net negative charge loss =  $+0.023e$ ). Consistent with this observation, the positive charge on Cd decreased from  $+11.227e$  (for the bare CdS) to  $+11.194e$  (net positive charge loss =  $-0.033e$ ), which indicates that an electron transfer occurred from the N atom of the amine to the Cd of CdS. The residual charges on S and Cd of CdS QDs were the main source of the radiative recombination surface state centers; therefore, the changes in the residual charges on S and Cd of CdS clusters, which resulted from organic molecular adsorption, can directly alter the quantity of these radiative surface states on QDs. Thus, in the case of the typical CdS-BA system, the decreased positive charge on Cd can downsize electron surface states, which reduces the surface-related emission, the longer lifetime component, and eventually, the overall PL-QY. Conversely, the net gain of negative charge on S, which can multiply hole surface states, predicts higher surface-related emission with an increased longer lifetime component and higher overall PL-QY, which is in contrast to the experimental observations, indicating that hole surface states-related phenomena do not occur. This occurred because, although abundant quantities of photoexcited holes were available on the organics-modified QDs surface, fewer electron surface states and photoexcited electrons necessary for radiative electron-hole recombination were available on the CdS QDs surface because of the decreased Cd atom positive charge, thereby preventing such an increase of PL-QY.

The proposed mechanism can be extended to explain the behavior of the other amine, *n*-HA, and the acid OA towards decreasing the longer lifetime component of photoexcited charges and the PL-QY of CdS QDs. Notably, the acid OA caused more changes compared to the amines, despite the fact that OA had low binding energy ( $-0.13$  eV, Table 2), and weakly adsorbed on the CdS in comparison to the amines. Table 3 shows that the positive charge loss on Cd was the highest ( $-0.043e$ ) by the OA molecule, compared to BA ( $-0.033e$ ) and HA ( $-0.020e$ ). Consequently, more electron surface states can be reduced on the surface by OA, and this trend of decreasing electron surface states is consistent with the decreasing longer lifetime component and lower PL-QY by this ligand. This confirms that the net charge transfer between the organic molecule and the CdS QDs is the crucial factor, rather than the binding energy of the molecule, in effecting the carrier recombination dynamics by controlling the radiative recombination surface state centers.

## 5. Conclusion

Based on the TRPL analysis and DFT computation, this study demonstrated that the amine can be used as the capping ligands for CdSe QDs to enhance PL-QYs, whereas the amine used as the capping ligands for CdS QDs can be used to PL-QYs. The PL-QYs of CdSe and CdS QDs decreased considerably when using oleic acid as capping ligands. We propose that the interactions between capping ligands and CdSe or CdS QDs may be attributed to  $\text{NH}_2$  group for amine molecules and  $-\text{COOH}$  group for fatty acid molecules. An improved understanding of this interaction will facilitate the design of superior conjugates for CdSe and CdS QDs for various applications.



## Author details

Liang-Yih Chena\* and Chia-Hung Tseng

*Department of Chemical Engineering, National Taiwan University of Science and Technology, Taipei, Taiwan*

Hung-Lung Chou

*Graduate Institute of Applied Science and Technology, National Taiwan University of Science and Technology, Taipei, Taiwan*

Ching-Hsiang Chen

*Protrustech Corporation Limited, Tainan, Taiwan*

## Acknowledgement

We thank the NCHC HPC and NTUST for providing massive computing time. Financially support from the National Science Council under Contract No. NSC 99-2811-M-011-005 is gratefully acknowledged.

## 6. References

- [1] G. Markovich, C. P. Collier, S. E. Henrichs, F. Remacle, R. D. Levine, and J. R. Heath (1999) Architectonic Quantum Dot Solids. *Acc. Chem. Res.* 32: 415-423.
- [2] A. P. Alivisatos (1996) Semiconductor Clusters, Nanocrystals, and Quantum Dots *Science.* 271: 933-937.
- [3] M. Bruchez, M. M. Jr., P. Gin, S. Weiss, and A. P. Alivisatos (1998) Semiconductor Nanocrystals as Fluorescent Biological Labels *Science.* 281: 2013-2016.
- [4] W. C. W. Chan and S. Nie (1998) Quantum Dot Bioconjugates for Ultrasensitive Nonisotopic Detection *Science.* 281: 2016-2018.
- [5] J. Hranisavljevic, N. M. Dimitrijevic, G. A. Wurtz, and G. P. Wiederrecht (2002) Photoinduced Charge Separation Reactions of J-Aggregates Coated on Silver Nanoparticles. *J. Am. Chem. Soc.* 124: 4536-4537.
- [6] J. K. Jaiswal, H. Mattoussi, J. M. Mauro, and S. M. Simon (2003) Long-term Multiple Color Imaging of Live Cells Using Quantum Dot Bioconjugates *Nat. Biotechnol.* 21: 47-51.
- [7] S. Kim, Y. T. Lim, E. G. Soltész, A. M. D. Grand, J. Lee, A. Nakayama, J. A. Parker, T. Mihaljevic, R. G. Laurence, D. M. Dor, L. H. Cohn, M. G. Bawendi, and J. V. Frangioni (2004) Near-Infrared Fluorescent Type II Quantum Dots for Sentinel Lymph Node mapping *Nat. Biotechnol.* 22: 93-97.
- [8] X. Gao, Y. Cui, R. M. Levenson, L. W. K. Chung, and S. Nie (2004) In Vivo Cancer Targeting and Imaging with Semiconductor Quantum Dots *Nat. Biotechnol.* 22: 969-976.

---

\* Corresponding Author

- [9] W. U. Huynh, X. Peng, and A. P. Alivisatos (1999) CdSe Nanocrystal Rods/Poly(3-hexylthiophene) Composite Photovoltaic Devices. *Adv. Mater.* 11: 923-927.
- [10] W. U. Huynh, J. J. Dittmer, and A. P. Alivisatos (2002) Hybrid Nanorod-Polymer Solar Cells *Science*. 295: 2425-2427.
- [11] R. D. Schaller and V. I. Klimov (2004) High Efficiency Carrier Multiplication in PbSe Nanocrystals: Implications for Solar Energy Conversion. *Phys. Rev. Lett.* 92: 186601-1~186601-4.
- [12] J. Liu, T. Tanaka, K. Sivula, A. P. Alivisatos, and J. M. J. Fréchet (2004) Employing End-Functional Polythiophene To Control the Morphology of Nanocrystal-Polymer Composites in Hybrid Solar Cells. *J. Am. Chem. Soc.* 126: 6550-6551.
- [13] R. J. Ellingson, M. C. Beard, J. C. Johnson, P. Yu, O. I. Micic, A. J. Nozik, A. Shabaev, and A. L. Efros (2005) Highly Efficient Multiple Exciton Generation in Colloidal PbSe and PbS Quantum Dots. *Nano Lett.* 5: 865-871.
- [14] W. Cai, D.-W. Shin, K. Chen, O. Gheysens, Q. Cao, S. X. Wang, S. S. Gambhir, and X. Chen (2006) Peptide-Labeled Near-Infrared Quantum Dots for Imaging Tumor Vasculature in Living Subjects. *Nano Lett.* 6: 669-676.
- [15] N. J. Smith, K. J. Emmett, and S. J. Rosenthal (2008) Photovoltaic Cells Fabricated by Electrophoretic Deposition of CdSe Nanocrystals *Appl. Phys. Lett.* 93: 043504.
- [16] B. O. Dabbousi, M. G. Bawendi, O. Onitsuka, and M. F. Rubner (1995) Electroluminescence from CdSe Quantum-Dot/Polymer Composites. *Appl. Phys. Lett.* 66: 1316.
- [17] M. C. Schlamp, X. Peng, and A. P. Alivisatos (1997) Improved Efficiencies in Light Emitting Diodes made with CdSe(CdS) Core/Shell type Nanocrystals and a Semiconducting Polymer. *J. Appl. Phys.* 82: 5837.
- [18] H. Mattoussi, L. H. Radzilowski, B. O. Dabbousi, E. L. Thomas, M. G. Bawendi, and M. F. Rubner (1998) Electroluminescence from Heterostructures of Poly(phenylene vinylene) and Inorganic CdSe Nanocrystals *J. Appl. Phys.* 83: 7965.
- [19] S. Coe, W.-K. Woo, M. Bawendi, and V. Bulovi (2002) Electroluminescence from Single Monolayers of Nanocrystals in Molecular Organic Devices *Nature*. 420: 800-803.
- [20] R. A. M. Hikmet, P. T. K. Chin, D. V. Talapin, and H. Weller (2005) Polarized-Light-Emitting Quantum-Rod Diodes. *Adv. Mater.* 17: 1436-1439.
- [21] A. H. Mueller, M. A. Petruska, M. Achermann, D. J. Werder, E. A. Akhador, D. D. Koleske, M. A. Hoffbauer, and V. I. Klimov (2005) Multicolor Light-Emitting Diodes Based on Semiconductor Nanocrystals Encapsulated in GaN Charge Injection Layers. *Nano Lett.* 5: 1039-1044.
- [22] J. Zhao, J. A. Bardecker, A. M. Munro, M. S. Liu, Y. Niu, I. K. Ding, J. Luo, B. Chen, A. K. Y. Jen, and D. S. Ginger (2006) Efficient CdSe/CdS Quantum Dot Light-Emitting Diodes Using a Thermally Polymerized Hole Transport Layer. *Nano Lett.* 6: 463-467.
- [23] P. O. Anikeeva, C. F. Madigan, J. E. Halpert, M. G. Bawendi, and V. Bulović (2008) Electronic and Excitonic Processes in Light-Emitting Devices Based on Organic Materials and Colloidal Quantum Dots. *Phys. Rev. B.* 78: 085434.
- [24] A. P. Alivisatos (1996) Perspectives on the Physical Chemistry of Semiconductor Nanocrystals. *J. Phys. Chem.* 100: 13226-13239.

- [25] M. Marandi, N. Taghavinia, A. Iraj, and S. M. Mahdavi (2005) A Photochemical Method for Controlling the Size of CdS Nanoparticles. *Nanotechnology*. 16: 334-338.
- [26] W. W. Yu and X. Peng (2002) Formation of High-Quality CdS and Other II-VI Semiconductor Nanocrystals in Noncoordinating Solvents: Tunable Reactivity of Monomers. *Angew Chem. Int. Ed.* 41: 2368-2371.
- [27] D. Pan, S. Jiang, L. An, and B. Jiang (2004) Controllable Synthesis of Highly Luminescent and Monodisperse CdS Nanocrystals by a two-Phase Approach under Mild Conditions. *Adv. Mater.* 16: 982-985.
- [28] J. He, J. Mi, H. Li, and W. Ji (2005) Observation of Interband Two-Photon Absorption Saturation in CdS Nanocrystals. *J. Phys. Chem. B.* 109: 19184-19187.
- [29] J. Ouyang, J. Kuijper, S. Brot, D. Kingston, X. Wu, D. M. Leek, M. Z. Hu, J. A. Ripmeester, and K. Yu (2009) Photoluminescent Colloidal CdS Nanocrystals with High Quality via Noninjection One-Pot Synthesis in 1-Octadecene. *J. Phys. Chem. C.* 113: 7579-7593.
- [30] C. B. Murray, D. J. Norris, and M. G. Bawendi (1993) Synthesis and characterization of nearly monodisperse CdE (E = sulfur, selenium, tellurium) semiconductor nanocrystallites. *J. Am. Chem. Soc.* 115: 8706-8715.
- [31] M. E. Wankhede and S. K. Haram (2003) Synthesis and Characterization of Cd-DMSO Complex Capped CdS Nanoparticles. *Chem. Mater.* 15: 1296-1301.
- [32] E. Jang, S. Jun, Y. Chung, and L. Pu (2004) Surface Treatment to Enhance the Quantum Efficiency of Semiconductor Nanocrystals. *J. Phys. Chem. B.* 108: 4597-4600.
- [33] P. Thangadurai, S. Balaji, and P. T. Manoharan (2008) Surface Modification of CdS Quantum Dots Using Thiols—Structural and Photophysical Studies *Nanotechnology*. 19: 435708-1~435708-8.
- [34] J. Aldana, Y. A. Wang, and X. Peng (2001) Photochemical Instability of CdSe Nanocrystals Coated by Hydrophilic Thiols. *J. Am. Chem. Soc.* 123: 8844-8850.
- [35] D. V. Talapin, A. L. Rogach, A. Kornowski, M. Haase, and H. Weller (2001) Highly Luminescent Monodisperse CdSe and CdSe/ZnS Nanocrystals Synthesized in a Hexadecylamine-Trioctylphosphine Oxide-Trioctylphosphine Mixture. *Nano Lett.* 1: 207-211.
- [36] V. Swayambunathan, D. Hayes, K. H. Schmidt, Y. X. Liao, and D. Meisel (1990) Thiol surface complexation on growing cadmium sulfide clusters. *J. Am. Chem. Soc.* 112: 3831-3837.
- [37] T. Uchihara, S. Maedomari, T. Komesu, and K. Tanaka Influences of Proton-Dissociation Equilibrium of Capping Agents on the Photo-Chemical Events of the Colloidal Solutions Containing the Thiol-Capped Cadmium Sulfide Particles *J. Photochem. and Photobio.* 161: 227-232.
- [38] X. Peng, T. E. Wilson, A. P. Alivisatos, and P. G. Schultz (1997) Synthesis and Isolation of a Homodimer of Cadmium Selenide Nanocrystals. *Angew Chem. Int. Ed.* 36: 145-147.
- [39] S. Pathak, S.-K. Choi, N. Arnheim, and M. E. Thompson (2001) Hydroxylated Quantum Dots as Luminescent Probes for in Situ Hybridization. *J. Am. Chem. Soc.* 123: 4103-4104.
- [40] G. Kalyuzhny and R. W. Murray (2005) Ligand Effects on Optical Properties of CdSe Nanocrystals. *J. Phys. Chem. B.* 109: 7012-7021.

- [41] C. Bullen and P. Mulvaney (2006) The Effects of Chemisorption on the Luminescence of CdSe Quantum Dots. *Langmuir*. 22: 3007-3013.
- [42] A. M. Munro, I. J.-L. Plante, M. S. Ng, and D. S. Ginger (2007) Quantitative Study of the Effects of Surface Ligand Concentration on CdSe Nanocrystal Photoluminescence. *J. Phys. Chem. C*. 111: 6220-6227.
- [43] S. A. Gallagher, M. P. Moloney, M. Wojdyla, S. J. Quinn, J. M. Kelly, and Y. K. Gun'ko (2010) Synthesis and Spectroscopic Studies of Chiral CdSe Quantum Dots *J. Mater. Chem.* 20: 8350-8355.
- [44] O. Chen, Y. Yang, T. Wang, H. Wu, C. Niu, J. Yang, and Y. C. Cao (2011) Surface-Functionalization-Dependent Optical Properties of II-VI Semiconductor Nanocrystals. *J. Am. Chem. Soc.* 133: 17504-17512.
- [45] G. Kalyuzhny and R. W. Murray. (2005) Ligand Effects on Optical Properties of CdSe Nanocrystals. *J. Phys. Chem. B*. 109: 7012-7021.
- [46] A. Hoshino, K. Fujioka, T. Oku, M. Suga, Y. F. Sasaki, T. Ohta, M. Yasuhara, K. Suzuki, and K. Yamamoto (2004) Physicochemical Properties and Cellular Toxicity of Nanocrystal Quantum Dots Depend on Their Surface Modification. *Nano Lett.* 4: 2163-2169.
- [47] T. Tsuruoka, K. Akamatsu, and H. Nawafune (2004) Synthesis, Surface Modification, and Multilayer Construction of Mixed-Monolayer-Protected CdS Nanoparticles. *Langmuir*. 20: 11169-11174.
- [48] F. Dubois, B. Mahier, B. Dubertret, E. Doris, and C. Mioskowski (2006) A Versatile Strategy for Quantum Dot Ligand Exchange. *J. Am. Chem. Soc.* 129: 482-483.
- [49] H.-L. Chou, C.-H. Tseng, K. C. Pillai, B.-J. Hwang, and L.-Y. Chen (2010) Adsorption and Binding of Capping Molecules for Highly Luminescent CdSe Nanocrystals - DFT Simulation Studies. *Nanoscale*. 2: 2679-2684.
- [50] M. Jones and G. D. Scholes (2010) On the use of Time-Resolved Photoluminescence as a Probe of Nanocrystal Photoexcitation Dynamics *J. Mater. Chem.* 20: 3533.
- [51] G. Schlegel, J. Bohnenberger, I. Potapova, and A. Mews (2002) Fluorescence Decay Time of Single Semiconductor Nanocrystals. *Phys. Rev. Lett.* 88: 137401.
- [52] M. Nirmal, D. J. Norris, M. Kuno, M. G. Bawendi, A. L. Efros, and M. Rosen (1995) Observation of the "Dark Exciton" in CdSe Quantum Dots. *Phys. Rev. Lett.* 75: 3728-3731.
- [53] X. Wang, L. Qu, J. Zhang, X. Peng, and M. Xiao (2003) Surface-Related Emission in Highly Luminescent CdSe Quantum Dots. *Nano Lett.* 3: 1103-1106.
- [54] M. Jones, S. Kumar, S. S. Lo, and G. D. Scholes (2008) Exciton Trapping and Recombination in Type II CdSe/CdTe Nanorod Heterostructures. *J. Phys. Chem. C*. 112: 5423-5431.
- [55] B. L. Wehrenberg, C. Wang, and P. Guyot-Sionnest (2002) Interband and Intraband Optical Studies of PbSe Colloidal Quantum Dots. *J. Phys. Chem. B*. 106: 10634-10640.
- [56] A. I. Ekimov, F. Hache, M. C. Schanne-Klein, D. D. Ricard, C. Flytzanis, I. A. Kudryavtsev, T. V. Yazeva, A. V. Rodina, and A. L. Efros (1993) Absorption and Intensity-Dependent Photoluminescence Measurements on CdSe Quantum Dots: Assignment of the First Electronic Transitions. *J. Opt. Soc. Am. B*. 10: 100-107.

- [57] S. Pokrant and K. B. Whaley (1999) Tight-Binding Studies of Surface Effects on Electronic Structure of CdSe Nanocrystals: the Role of Organic Ligands, Surface Reconstruction, and Inorganic Capping Shells. *Eur. Phys. J. D.* 6: 255-267.
- [58] L.-W. Wang and A. Zunger (1996) Pseudopotential Calculations of Nanoscale CdSe Quantum Dots. *Phys. Rev. B.* 53: 9579-9582.
- [59] F. A. Reboledo and A. Zunger (2001) Surface-Passivation-Induced Optical Changes in Ge Quantum Dots. *Phys. Rev. B.* 63: 235314.
- [60] G. M. Dalpian, M. L. Tiago, M. L. d. Puerto, and J. R. Chelikowsky (2006) Symmetry Considerations in CdSe Nanocrystals. *Nano Lett.* 6: 501-504.
- [61] M. L. del Puerto, M. L. Tiago, and J. R. Chelikowsky (2006) Excitonic Effects and Optical Properties of Passivated CdSe Clusters. *Phys. Rev. Lett.* 97: 096401.
- [62] J. Y. Rempel, B. L. Trout, M. G. Bawendi, and K. F. Jensen (2006) Density Functional Theory Study of Ligand Binding on CdSe (0001), (000 $\bar{1}$ ), and (1120) Single Crystal Relaxed and Reconstructed Surfaces: Implications for Nanocrystalline Growth. *J. Phys. Chem. B.* 110: 18007-18016.
- [63] A. Puzder, A. J. Williamson, F. Gygi, and G. Galli (2004) Self-Healing of CdSe Nanocrystals: First-Principles Calculations. *Phys. Rev. Lett.* 92: 217401.
- [64] S. Kilina, S. Ivanov, and S. Tretiak (2009) Effect of Surface Ligands on Optical and Electronic Spectra of Semiconductor Nanoclusters. *J. Am. Chem. Soc.* 131: 7717-7726.
- [65] H. Kamisaka, S. V. Kilina, K. Yamashita, and O. V. Prezhdo (2008) Ab Initio Study of Temperature and Pressure Dependence of Energy and Phonon-Induced Dephasing of Electronic Excitations in CdSe and PbSe Quantum Dots. *J. Phys. Chem. C.* 112: 7800-7808.
- [66] H.-L. Chou, C.-H. Tseng, K. C. Pillai, B.-J. Hwang, and L.-Y. Chen (2011) Surface Related Emission in CdS Quantum Dots. DFT Simulation Studies. *J. Phys. Chem. C.* 115: 20856-20863.
- [67] R. G. Pearson (1963) Hard and Soft Acids and Bases. *J. Am. Chem. Soc.* 85: 3533-3539.
- [68] J. Chen, J. L. Song, X. W. Sun, W. Q. Deng, C. Y. Jiang, W. Lei, J. H. Huang, and R. S. Liu (2009) An Oleic Acid-Capped CdSe Quantum-Dot Sensitized Solar Cell Appl. *Phys. Lett.* 94: 153115.
- [69] P. Schapotschnikow, B. Hommersom, and T. J. H. Vlugt (2009) Adsorption and Binding of Ligands to CdSe Nanocrystals. *J. Phys. Chem. C.* 113: 12690-12698.